18th Brazilian Congress of Thermal Sciences and Engineering
November 16-20, 2020 (Online)

# ENC-2020-0621
# INFLUENCE OF WORKING FLUID ON THERMAL PERFORMANCE OF THERMOSYPHONS FOR APPLICATION IN HIGH PRESSURE VACUUM TUBE SOLAR COLLECTORS

**Guilherme Antonio Bartmeyer**[1]
**Victor Vaurek Dimbarre**[2]
**Pedro Leineker Ochoski Machado**[3]
**Thiago Antonini Alves**[4]
Federal University of Technology – Paraná, Academic Department of Mechanics
Doctor Washington Subtil Chueire street, 330, Jardim Carvalho, 84017-220, Ponta Grossa, PR, Brazil
gabartmeyer@hotmail.com[1], victorvaurek@gmail.com[2], pedmac@alunos.utfpr.edu.br[3], antonini@utfpr.edu.br[4]

**Paulo Henrique Dias dos Santos**[5]
Federal University of Technology – Paraná, Academic Department of Mechanics
Deputado Heitor Alencar Furtado street, 5000, Ecoville, 81280-340, Curitiba, PR, Brasil
psantos@utfpr.edu.br[5]

***Abstract.*** *Solar collectors are devices that absorb solar radiation and transfer it to a flowing fluid in order to heat it. One of the ways to increase the efficiency of these devices consists in using thermosyphons. Thermosyphons are highly efficient heat transfer devices which use latent heat of vaporization to transport high amounts of energy in the form of heat with a small temperature gradient. These devices consist basically in an evacuated metallic tube filled with a working fluid. Heat is absorbed in the evaporator region, generating steam from the working fluid. When the steam reaches the condenser region, heat is dissipated to the environment, condensing the steam that returns to the evaporator at the liquid state. In this work, different thermosyphons with three different working fluids (acetone, methanol, and distilled water) were built and tested. The evaporator and the adiabatic section have an outer diameter of 8.33mm and lengths of 1,600mm and 40mm, respectively. The condenser has an outer diameter of 13.40mm and a length of 35mm. The filling ratio used was 50% of the evaporator's volume. Tests were carried out discharging heat at the evaporator due to Joule's effect using a resistive tape and a power supply, while water flows at the condenser absorbing heat from it. Three different flow rates of water were used: 0.50, 0.75, and 1.00 L/min. Thermocouples were placed along the devices in order to obtain temperature data. The thermal analysis was based in temperature distribution, thermal resistance, and thermal efficiency. Acetone was found out as the working fluid with best performance along the three working fluids tested. Concerning the influence of the flow rate of water, higher flow rates equals lower temperatures along the devices and higher thermal efficiencies.*

***Keywords:*** *Thermosyphon, Heat Pipe, Heat Transfer, Solar Collector.*

## 1. INTRODUCTION

Brazil has a high energy potential when it comes to solar generation. This is due to the fact that most of its territory is located in the subtropical region, since the intensity of the sun's rays depends on the geographic latitude of the area in question and the season (Pereira et al., 2017). One of the ways to utilize that energy is called solar collector. These devices are a type of heat exchanger that converts solar radiation into thermal energy. In other words, it's a device that absorb the solar radiation and transfers it to a flowing fluid in order to heat it. Higher outlet temperatures are obtained with higher collector efficiencies, where higher heat is transferred to the fluid (Shukla et al., 2013).

An alternative developed in order to increase the efficiency of these devices are the Thermosyphon Heat Pipe Evacuated Tube Collectors (*THPETC*) or Heat Pipe Solar Collectors (*HPSC*) (Kalogirou, 2004). Thermosyphons are highly efficient heat transfer devices which utilize latent heat of vaporization to transport high amounts of energy in the form of heat with a small temperature gradient. These devices consist basically in an evacuated metallic tube filled with a working fluid (Peterson, 1994; Faghri, 2014; Reay et al., 2014).

The thermosyphon has three regions with different functions in their operation, they are: evaporator, adiabatic section, and condenser. The evaporator, the lower region of the thermosyphon, is heated using a hot source and the working fluid undergoes an evaporation process. This steam, due to pressure difference, moves to the coldest region of the thermosyphon (condenser). In the condenser, the vapor generated loses energy and is condensed. The working fluid

in the liquid state returns to the evaporator, by gravity, closing the thermodynamic cycle. The adiabatic section is located between the evaporator and the condenser, in this region there is no heat exchange between the thermosyphon and the environment and in some cases the adiabatic region is non-existent (Mantelli, 2013). A schematic diagram of the thermosyphon operating principle is shown in Figure 1.

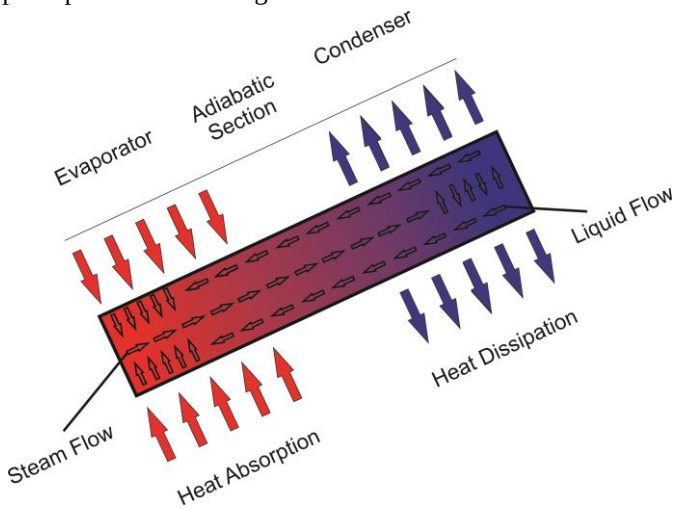


Figure 1. Schematic diagram of a thermosyphon.

The advantages of application of this devices to solar collectors consist in the thermosyphon's high heat transfer capacity and it also removes obstacles encountered in other applications such as freezing and overheating. In the *THPETC* the heat losses by convection and conduction are minimized be the vacuum envelope, achieving a higher energetic efficiency and higher temperatures than the usual flat plate collectors (Kalogirou, 2004; Riffat et al., 2005; Esroz, 2016).

Taking account into the principle of the different kinds of solar collectors, in the conventional ones (flat plates) heat is absorbed in the absorber plate and then transferred to the fluid, so there's a higher amount of mass that should be heated in order to heat the fluid. In the Heat Pipe Solar Collectors the heat exchange occurs by evaporation, condensation, and convection at higher effectivity levels and dispending a lower amount of time, justifying the use of those devices (Riffat et al., 2005; Esroz, 2016).

There are various parameters that can affect the efficiency of a *THPETC*, such as geometry, working fluid, filling ratio, and solar irradiation. Among these, the thermophysical properties of the working fluid are directly related to the proper functioning of this device. Vapor pressure, stability, toxicity, thermal conductivity, chemical compatibility between the working fluid, and the tube shell material must be taken into account, being the operating temperature range one of the first considerations that must be made when choosing the working fluid (Reay et al., 2014; Esroz, 2016).

Considering that, this present work intends to compare the performance of thermosyphons for application in *THPETC* operating with different working fluids under the same conditions. By that, it can be seen which working fluid provides the best results for use in that application, allowing the development of a more efficient *THPETC* and heating of water using clean energy. The influence of the flow rate of water in the condenser was also investigated. In order to compare the working fluids and flow rates, an experimental thermal analysis was made for each thermosyphon. Experimental data were verified and results discussed.

## 2. METHODOLOGY

This section presents the apparatus and proceedings intended to be used in order to achieve the main goal of this work.

### 2.1 Experimental Apparatus

The experimental apparatus used in this study is shown in Fig. 2 (a) and was composed of a *Politerm$^{TM}$16E* power supply (A), an *Agilent$^{TM}$ 34970A* data acquisition system with an *Agilent$^{TM}$ 34901A* 20-channel multiplexer (B), a *SOLAB$^{TM}$ SL-130* ultra-thermostatic bath (C), a *Dell$^{TM}$* portable microcomputer (D), a *UPS NHS$^{TM}$* (E), and an *Omega Engineering$^{TM}$ FL-2051* variable area flowmeter with regulating valve (F).

For the thermal analysis, the entire length of the evaporator was covered with a high thermal conductivity *Kapton$^{TM}$* tape and a total of eight *Omega Engineering$^{TM}$* type K thermocouples where distributed along the thermosyphon, one at the condenser, one at the adiabatic section, and six at the evaporator (equally spaced). The temperature data were collected every ten seconds using the data acquisition system.

At the evaporator, a resistive tape was wrapped in its whole length and connected with the power supply. The condenser was placed inside a 50mm diameter polyvinyl chloride tee that acts as a manifold. Through flexible connections and hoses, the tee was connected to the ultra-thermostated bath, allowing water to flow over the external surface of the condenser. The entire length of the evaporator and adiabatic region were isolated from the external environment with aeronautical thermal insulation and a polyethylene layer. The thermosyphon's configuration can be seen in Fig. 2 (b).

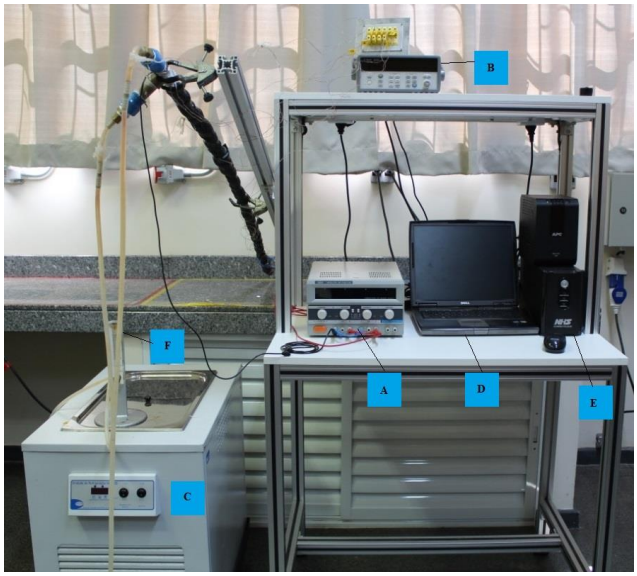


(a)

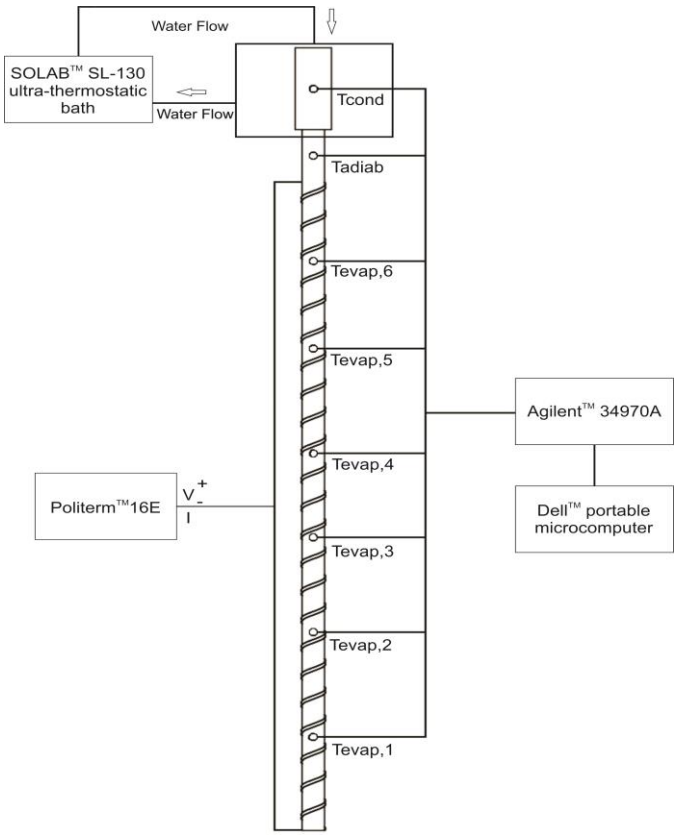


(b)

Figure 2. (a) Experimental apparatus and (b) thermosyphon's configuration.

## 2.2 Experimental Procedure

The thermosyphons were manufactured from a copper *ASTM B-75* tube with a total length of 1,675mm. The evaporator and the adiabatic section have an outer diameter of 8.33mm and lengths of 1,600mm and 40mm, respectively. The condenser has an outer diameter of 13.40mm and a length of 35mm. A total of three thermosyphons were made, each one filled with a different working fluid: acetone, distilled water, and methanol. All of them with filling rate of 50% of the evaporator volume. The methodology used in the construction of the thermosyphons (preparation, cleaning, assembly, tightness test, evacuation procedure, and filling with working fluid) was based on the information provided in Antonini Alves et al. (2018).

For the cleaning process every part of the thermosyphon was cleaned firstly using water and soup. After that, both caps, capillary tube, the connection (used to connect the adiabatic region and the condenser), and the condenser were subjected to an ultrasonic bath immersed in acetone. The interior of the wrapper was also cleaned using acetone. Finally, the ends of the wrapper, the connection, the two caps, and the capillary were bathed in a solution of sulfuric acid ($H_2SO_4$ 0.1M) for less than one minute. For assembly, all parts were joined by the tin brazing process. In the tightness test, using a positive displacement pump and a flexible hose, air was pumped into the thermosyphon while it was inside a recipient filled with water. If there was a fault, air bubbles would appear showing the flaws in the brazing, which would render the thermosyphon unable to operate.

After the tightness test the thermosyphon was connected to a vacuum pump in order to evacuate it. With the evacuation completed, a forceps was used to seal the hose, which was then removed from the vacuum pump and connected to a burette, allowing the thermosyphon to be filled with the desired amount of working fluid. After filling, a pressure plier was used to shape the capillary tube in order to prevent air from entering the device and, subsequently, the end of the capillary tube was brazed with tin in order to completely seal the thermosyphon.

For the tests, the evaporator is heated due to Joule's effect where the power supply dissipate power in the resistive tape, evaporating the working fluid. In the condenser, the water flow is responsible for the process of condensing the working fluid. The water used for the cooling process and the ambient temperature are maintained at 18.0°C ± 0.5°C by the ultra-thermostatic bath and a *Carrier*™ air conditioning system, respectively. Experimental tests were carried out for a heat load of 35 to 75W in a position at 25º from the horizontal (evaporator below condenser) corresponding to the latitude of the city of Ponta Grossa/PR/Brazil: 25°05'42" South and with three different flow rates of water: 0.50, 0.75, and 1.00 L/min. Each heat value was maintained for about one hour and every test was repeated three times in order to confirm the repeatability of the data.

## 3. RESULTS AND DISCUSSION

Figures 3 to 5 present the temperature distribution for the thermosyphon filled with acetone and for the water flow ratios of 0.50, 0.75, and 1.00 L/min, respectively.

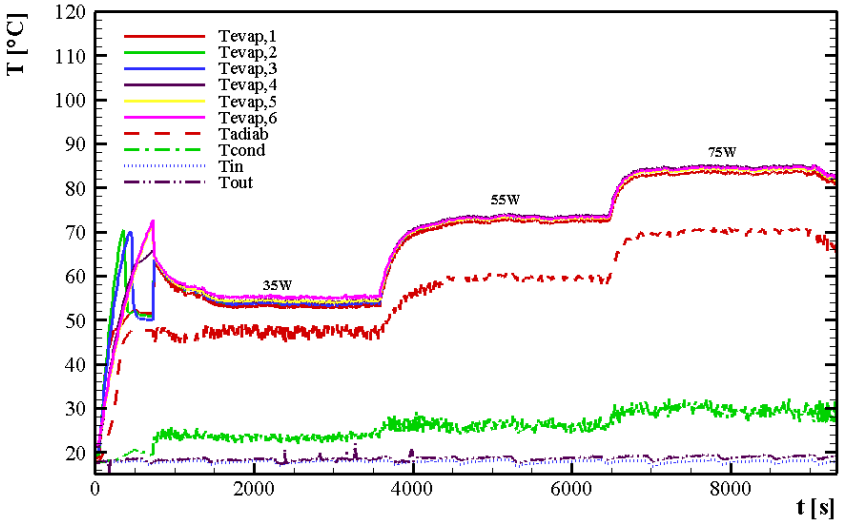


Figure 3. Temperature distribution for acetone at 0.50 L/min.

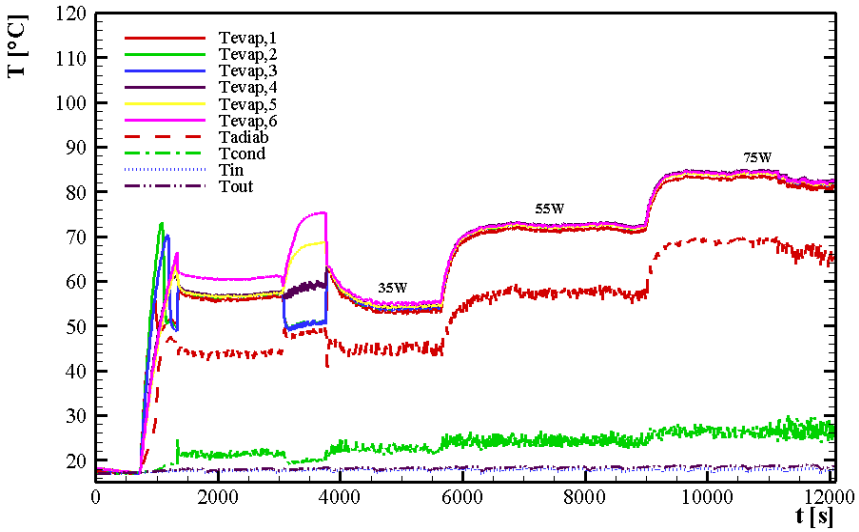


Figure 4. Temperature distribution for acetone at 0.75 L/min.

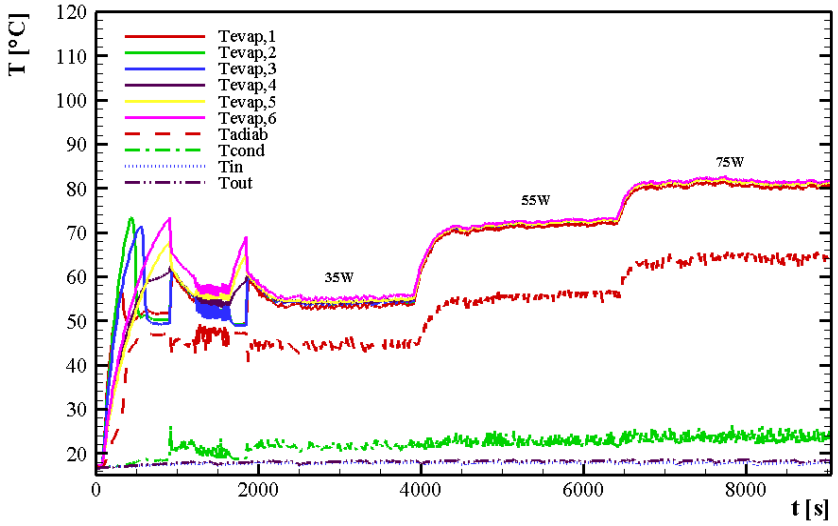


Figure 5. Temperature distribution for acetone at 1.00 L/min.

From Figures 3 to 5 it can be seen that for all flow rates of water the temperature distribution presented the same behavior, started to increase at first and then stabilized when reached steady state. At the heat load of 35W its noticed some instability at the temperature values. That instability may result from the fact that at first the lowest part of the thermosyphon presents a higher mass being heated than the rest of the evaporator, so, until there's a correspondence between the amount of working fluid being evaporated and the amount of steam being condensed, some parts of the evaporator may present higher temperatures, that can be seen in temperature peaks in Figs. 3 to 5 at the first heat load.

Table 1 presents the average temperature at steady state from each region of the device and each flow rate of water, and it can be seen that higher flow rate equals lower temperatures for every section at every heat load.

Table 1. Temperatures in [°C] obtained in a steady state for acetone as a working fluid.

| **Flow Rate** | | **35W** | | | **55W** | | | **75W** | |
|---|---|---|---|---|---|---|---|---|---|
| **[L/min]** | $T_{evap}$ | $T_{adiab}$ | $T_{cond}$ | $T_{evap}$ | $T_{adiab}$ | $T_{cond}$ | $T_{evap}$ | $T_{adiab}$ | $T_{cond}$ |
| **0.50** | 54.5 | 47.2 | 23.4 | 73.0 | 59.6 | 26.0 | 84.3 | 70.1 | 29.6 |
| **0.75** | 54.9 | 44.7 | 22.4 | 72.3 | 57.5 | 24.3 | 83.4 | 68.1 | 26.4 |
| **1.00** | 54.5 | 44.6 | 21.6 | 72.1 | 55.6 | 22.7 | 81.3 | 64.2 | 23.7 |

Figures 6 to 8 present the temperature distribution for the thermosyphon filled with methanol and for the flow ratios of 0.50, 0.75 and, 1.00 L/min, respectively. Comparing Figures 6 to 8 with Figures 3 to 5 it's noticed that temperature data for methanol presented a similar behavior from data for acetone. At first, there is a temperature equilibrium between each region and then, with the dissipation of the heat load temperature stars to rise until it reaches steady state. As it was expected, temperature from all the thermocouples at the evaporator region were higher than at the adiabatic region, that were also higher than temperature at the condenser. At the first heat load, instability was also observed, but less intense in a certain way. The reason for the instability remains the same, different values of mass to be heat at different regions of the device. The difference in temperature values and intensity of instability occurs due to different thermophysical properties of the fluids, such as thermal conductivity, surface tension, density, and viscosity.

Table 2 presents the average temperature at steady state from each region of the device and each flow rate.

Table 2. Temperatures in [°C] obtained in a steady state for methanol as a working fluid.

| **Flow Rate** | | **35W** | | | **55W** | | | **75W** | |
|---|---|---|---|---|---|---|---|---|---|
| **[L/min]** | $T_{evap}$ | $T_{adiab}$ | $T_{cond}$ | $T_{evap}$ | $T_{adiab}$ | $T_{cond}$ | $T_{evap}$ | $T_{adiab}$ | $T_{cond}$ |
| **0.50** | 57.6 | 49.6 | 25.5 | 75.0 | 59.4 | 30.2 | 91.3 | 74.4 | 33.2 |
| **0.75** | 62.1 | 47.9 | 24.9 | 79.0 | 62.7 | 29.6 | 91.6 | 75.6 | 34.5 |
| **1.00** | 62.4 | 45.6 | 22.5 | 77.5 | 58.9 | 25.0 | 89.6 | 71.2 | 28.7 |

Comparing Table 1 and Table 2, it can be observed that methanol presented higher values of temperature in every situation. Beyond that, increasing flow rate didn't resulted in a default behavior in temperatures such as occurred for acetone. Both facts may be explained by different thermophysical properties of the working fluid.

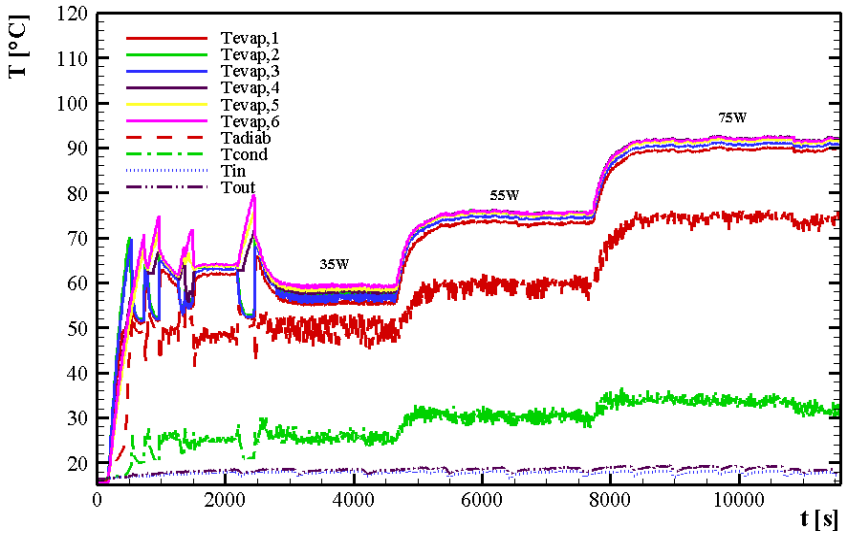


Figure 6. Temperature distribution for methanol at 0.50 L/min.

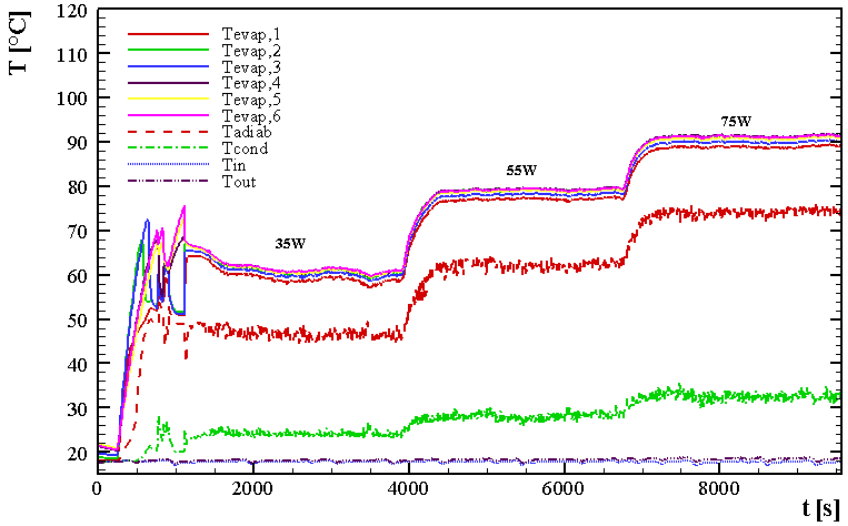


Figure 7. Temperature distribution for methanol at 0.75 L/min.

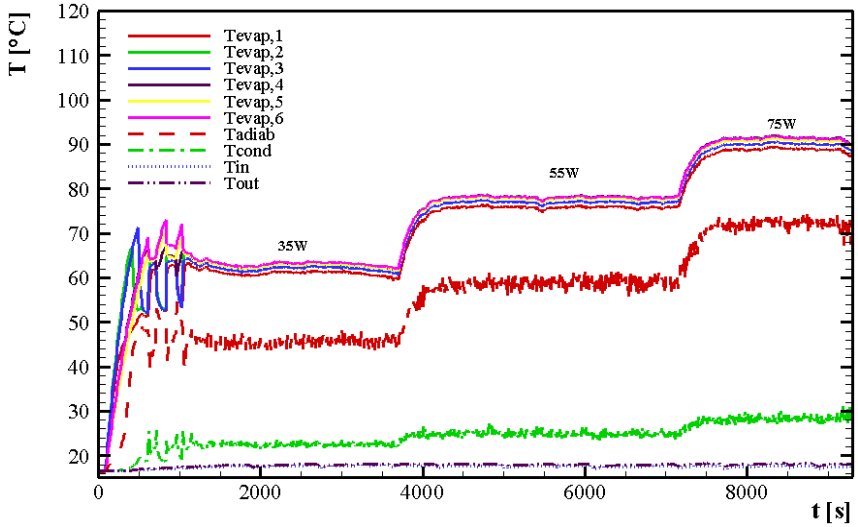


Figure 8. Temperature distribution for methanol at 1.00 L/min.

Figures 9 to 11 present the temperature distribution for the thermosyphon filled with distilled water and for the flow ratios of 0.50, 0.75, and 1.00 L/min, respectively.

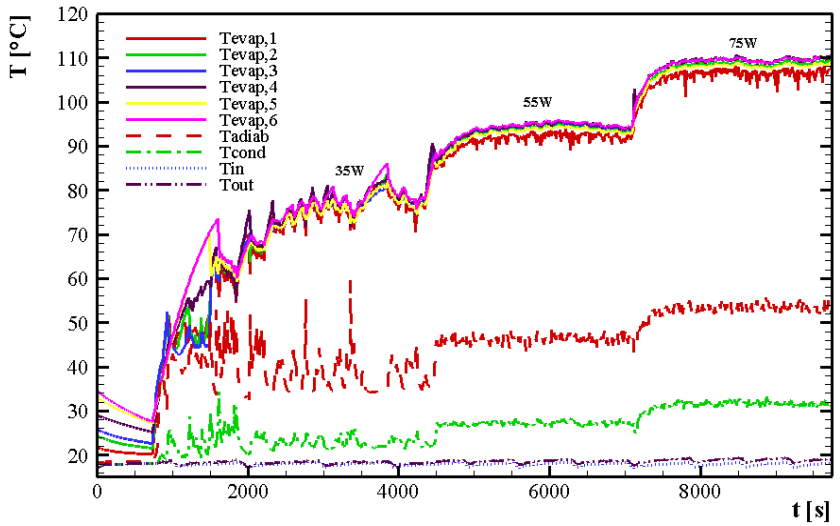


Figure 9. Temperature distribution for water at 0.50 L/min.

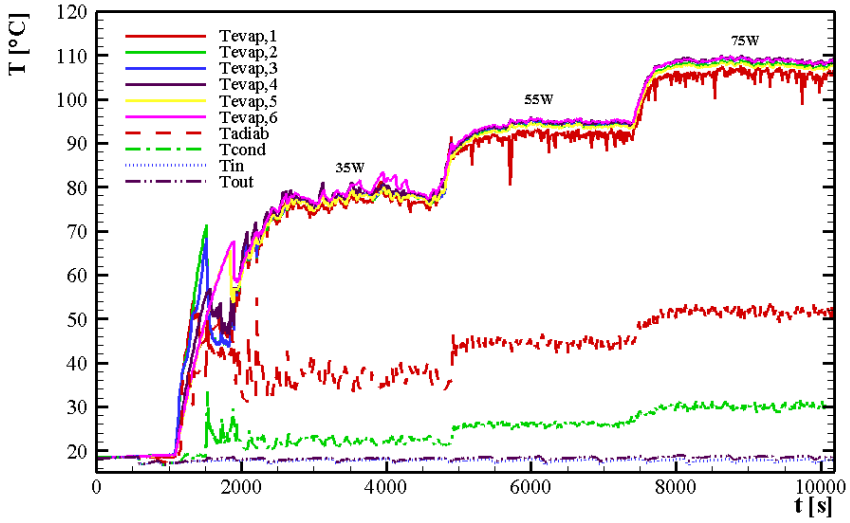


Figure 10. Temperature distribution for water at 0.75 L/min.

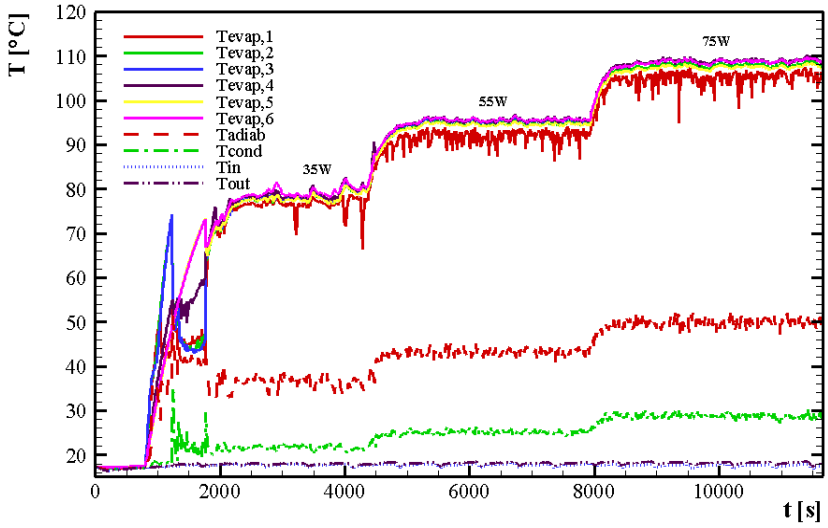


Figure 11. Temperature distribution for water at 1.00 L/min.

Once again the influence of the thermophysical properties of the working fluid can be observed. When filled with distilled water, the temperature distribution presented much more instabilities for all the heat loads applied and also all the flow rates. Comparing with the temperature distribution of the other two working fluids it can also be seen that results for distilled water presented higher temperatures in all the three regions of the thermosyphon in every case. This fact may indicate that distilled water presented the worst behavior compared to the other two working fluids, since lower temperatures may indicate a higher heat transfer trough the device. Table 3 presents the average temperature at steady state from each region of the device and each flow rate.

Table 3. Temperatures in [°C] obtained in a steady state for distilled water as a working fluid.

| **Flow Rate** | | **35W** | | | **55W** | | | **75W** | |
|---|---|---|---|---|---|---|---|---|---|
| **[L/min]** | $T_{evap}$ | $T_{adiab}$ | $T_{cond}$ | $T_{evap}$ | $T_{adiab}$ | $T_{cond}$ | $T_{evap}$ | $T_{adiab}$ | $T_{cond}$ |
| **0.50** | 75.5 | 38.4 | 22.9 | 93.8 | 46.3 | 27.2 | 108.6 | 53.5 | 31.7 |
| **0.75** | 77.9 | 36.8 | 22.3 | 93.8 | 44.6 | 26.0 | 108.0 | 51.6 | 30.1 |
| **1.00** | 78.2 | 36.4 | 21.7 | 94.7 | 43.2 | 25.2 | 107.8 | 50.0 | 28.8 |

Comparing Table 3 to Tables 1 and 2, it can be noticed that temperatures using distilled water as the working fluid resulted in higher temperatures in every section, and also higher gap between evaporator's temperature and condenser's temperature. In general, higher flow rates equal lower temperatures, just as the results from acetone.

The gap between evaporator's temperature ($T_{evap}$) and condenser's temperature ($T_{cond}$) may be a way to indicate which working fluid works better in that conditions, mostly due to the thermal resistance ($R_{th}$ – Eq. (1)). This parameter is inversely proportional to the head load ($q$) and lower values of $R_{th}$ are desired in oppose of higher values. Figure 12 presents values of $R_{th}$ for each working fluid.

$$R_{th} = \frac{(T_{evap} - T_{cond})}{q}, \tag{1}$$

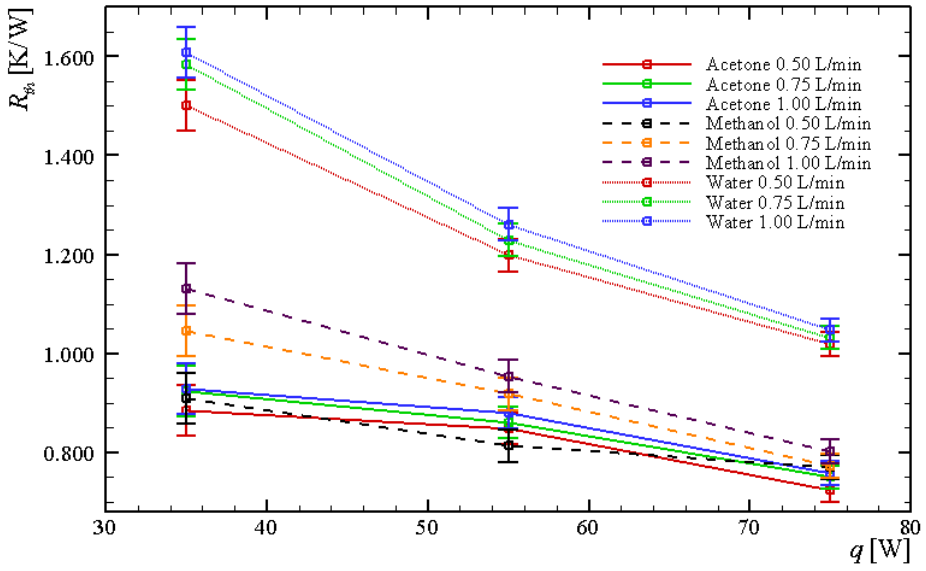


Figure 12. Thermal Resistance versus heat load.

From Figure 12 it can be noticed that higher flow rates equal higher values of $R_{th}$. Besides that, these values are consistent with data presented in Tables 1 to 3, since distilled water was the working fluid with higher gap between $T_{evap}$ and $T_{cond}$ and presented higher values of $R_{th}$ also. The behavior of thermal resistance for each working fluid acted as expected, since higher heat loads results in lower thermal resistance values, which indicates all thermosyphons were operating correctly.

In order to find out which working fluid operated better in the water heating process, the thermal efficiency ($\varepsilon_{ff}$) was calculated. It considers how much of the supplied energy ($q$) has been transferred to water ($Q$), and can be calculated by means of Eq. (2), in which $\dot{m}_{water}$ corresponds to the mass flow rate of water at the condenser, $c_p$ represents the specific heat, and $T_{out}$ and $T_{in}$ represents the water's temperature before and after the condenser. An average temperature between $T_{in}$ and $T_{out}$ was used as reference to achieve thermal physical properties of water. Table 4 presents values of thermal efficiency for all the working fluids.

$$\varepsilon_{ff} = \frac{Q}{q}100 = \frac{\dot{m}_{water}\, c_p (T_{out} - T_{in})}{q}100 . \quad (2)$$

Table 4. Thermal Efficiency.

| Working Fluid | Flow rate [L/min] | 35W $\varepsilon_{ff}$ [%] | 55W $\varepsilon_{ff}$ [%] | 75W $\varepsilon_{ff}$ [%] | Average $\varepsilon_{ff}$ [%] |
|---|---|---|---|---|---|
| **Acetone** | | 50.1 | 49.9 | 51.5 | 50.5 |
| **Methanol** | 0.50 | 49.6 | 49.2 | 45.2 | 48.0 |
| **Water** | | 34.2 | 42.4 | 47.0 | 41.2 |
| **Acetone** | | 49.8 | 50.6 | 51.5 | 50.6 |
| **Methanol** | 0.75 | 45.3 | 49.1 | 53.6 | 49.3 |
| **Water** | | 42.5 | 49.7 | 53.1 | 48.4 |
| **Acetone** | | 56.7 | 50.8 | 49.9 | 52.5 |
| **Methanol** | 1.00 | 53.7 | 46.3 | 53.7 | 51.2 |
| **Water** | | 48.0 | 52.0 | 55.9 | 52.0 |

From Table 4 it can be noticed that increasing flow rate, thermal efficiency is also increased. It can be justified by the fact that the convective coefficient is directly dependent of the flow velocity. Since the area remains the same, higher flow rate results in higher flow velocity and higher convective coefficient, promoting a greater heat transfer between the thermosyphon and the water. It can also be noticed that for every flow rate the working fluid that resulted in higher thermal efficiency was acetone. Observing Figure 12 it can be noticed that this result was already expected, since acetone presented the lowest value of thermal resistance for every flow rate.

From these results, it is concluded that the best working fluid among those analyzed for the desired working condition is acetone, since it was the working fluid that resulted in the lowest values of thermal resistance and also in higher thermal efficiency for all flow rates. Now, to continue the research, it is necessary to build a vacuum tube solar collector using acetone-filled thermosyphons in order to extract energy efficiency data and compare it with a commercial solar collector.

## 4. CONCLUSION

In this present work, thermosyphons with three different working fluids were build and tested in order to verify which one presents best performance in order to use it in a vacuum tube solar collector. The three tested thermosyphons presented same dimensions and same filling ratio. The working fluids investigated were acetone, methanol, and distilled water. For the comparison, heat load was discharged in the evaporator region due to Joule's effect using a resistive tape and a power supply, at the same time as heat was dissipated at the condenser region by means of a water flow. Three different flow rates of water were used in order to verify its influence on the devices' performance. Thermocouples were placed along the thermosyphons aiming to collect temperature data at the three regions of the devices. The thermal analysis was based in the temperature distribution, thermal resistance, and thermal effectivity of the three devices. The results showed that acetone presented the lowest temperature at the three regions for every heat load and every flow rate, followed by methanol and distilled water. It was possible to notice that higher flow rates induced lower temperatures at the devices and higher thermal efficiency. Since acetone presented the best results at the three thermal analysis parameters, it was chosen as the best working fluid for application in high pressure vacuum tube solar collectors.

## 5. ACKNOWLEDGEMENTS

Acknowledgments are provided to the Capes, the CNPq, the PROPPG/UTFPR, the DIRPPG/UTFPR, the PPGEM/ UTFPR/PG, and the DAMEC/UTFPR/PG.

## 6. REFERENCES

Antonini Alves, T., Krambeck, L. and Santos, P.H.D., 2018. "Heat Pipe and Thermosyphon for Thermal Management of Thermoelectric Cooling". In: Aranguren, P. (Org.). *Bringing Thermoelectricity into Reality*. InTech, London, UK.

Ersoz, M.A., 2016. "Effects of different working fluid use on the energy and exergy performance for evacuated tube solar collector with thermosyphon heat pipe". *Renewable Energy*, Vol. 96, pp. 244–256.

Faghri, A., 2014. "Heat pipes: review, opportunities and challenges". *Frontiers in Heat Pipes*, Vol. 5, No. 1.

Kalogirou, S.A. 2004. "Solar thermal collectors and applications". *Progress in Energy and Combustion Science*, Vol. 30, No. 3, pp. 231–295.

Mantelli, M.B.H., 2013. "Thermosyphon Technology for Industrial Applications". In: Vasiliev, L.L. and Kakaç, S. (Eds.). *Heat Pipes and Solid Sorption Transformations: Fundamentals and Practical Applications*. CRC Press, Boca Raton, USA.

Pereira, E.B., Martins, F.R., Gonçalves, A.R., Costa, R.S., Lima F.J.L., Rüther, R., Abreu, S.L., Tiepolo, G.M., Pereira, S.V. e Souza, J.G., 2017. *Atlas Brasileiro de Energia Solar*. Instituto Nacional de Pesquisas Espaciais, São José dos Campos, BRA.

Peterson, G. P., 1994. *An Introduction to Heat Pipes: Modeling, Testing and Application*. John Wiley & Sons, New York, USA.

Reay, D.A., Kew, P.A. and McGlen, R.J., 2014. *Heat Pipe: Theory, Design and Applications*. Butterworth-Heinemann, Amsterdam, NED.

Riffat, S.B., Zhao, X. and Doherty, P.S., 2005. "Developing a theoretical model to investigate thermal performance of a thin membrane heat-pipe solar collector". *Applied Thermal Engineering*, Vol. 25, pp. 899–915.

Shukla R., Sumathy, K., Erickson, P. and Gong, J., 2013. "Recent advances in the solar water heating systems: A review". *Renewable and Sustainable Energy Reviews*, Vol. 19, pp. 173–190.

## 7. RESPONSIBILITY NOTICE

The authors are the only responsible for the printed material included in this paper.